

ON THE HELICITY OF OPEN MAGNETIC FIELDS

C. PRIOR AND A. R. YEATES

Department of Mathematical Sciences, Durham University, Durham, DH1 3LE, UK; anthony.yeates@durham.ac.uk

Received 2014 January 24; accepted 2014 April 10; published 2014 May 7

ABSTRACT

We reconsider the topological interpretation of magnetic helicity for magnetic fields in open domains, and relate this to the relative helicity. Specifically, our domains stretch between two parallel planes, and each of these ends may be magnetically open. It is demonstrated that, while the magnetic helicity is gauge-dependent, its value in any gauge may be physically interpreted as the average winding number among all pairs of field lines with respect to some orthonormal frame field. In fact, the choice of gauge is equivalent to the choice of reference field in the relative helicity, meaning that the magnetic helicity is no less physically meaningful. We prove that a particular gauge always measures the winding with respect to a fixed frame, and propose that this is normally the best choice. For periodic fields, this choice is equivalent to measuring relative helicity with respect to a potential reference field. However, for aperiodic fields, we show that the potential field can be twisted. We prove by construction that there always exists a possible untwisted reference field.

Key words: magnetohydrodynamics (MHD) – methods: analytical – methods: numerical – Sun: magnetic fields

Online-only material: color figures

1. INTRODUCTION

Magnetic helicity $H(\mathbf{B}) = \int_V \mathbf{A} \cdot \mathbf{B} d^3x$ has long been recognized as an important dynamical invariant in ideal magnetohydrodynamics, with applications ranging from laboratory plasmas to astrophysical objects (Brown et al. 1999). Here \mathbf{A} is a vector potential for the magnetic field $\mathbf{B} = \nabla \times \mathbf{A}$, and it is a fundamental property of $H(\mathbf{B})$ that the integral is independent of the particular gauge chosen for \mathbf{A} , provided that V is simply connected and magnetically closed ($B_n = 0$ on the boundary ∂V). Analogous invariants exist for other solenoidal vector fields, notably the vorticity in fluid mechanics (Moffatt 1969).

Physically, $H(\mathbf{B})$ may be interpreted as a measure of the average topological linking of the magnetic field lines of \mathbf{B} (Moffatt 1969; Arnol'd 1986; Arnol'd & Khesin 1998). One way to see this is to consider a special magnetic configuration where \mathbf{B} is confined to two (or more) linked magnetic flux tubes that are closed and untwisted (see, for example, Moffatt & Ricca 1992). Another way is to write \mathbf{A} in Coulomb gauge ($\nabla \cdot \mathbf{A} = 0$), whence, providing that $B_n = 0$ on the whole boundary of V , it has the expression

$$\mathbf{A}(\mathbf{x}) = \frac{1}{4\pi} \int_V \frac{\mathbf{B}(\mathbf{y}) \times \mathbf{r}}{|\mathbf{r}|^3} d^3y, \quad (1)$$

where $\mathbf{r} = \mathbf{x} - \mathbf{y}$ (Cantarella et al. 2001). It follows that $H(\mathbf{B})$ may be written as

$$H(\mathbf{B}) = \frac{1}{4\pi} \int_V \int_V \mathbf{B}(\mathbf{x}) \cdot \frac{\mathbf{B}(\mathbf{y}) \times \mathbf{r}}{|\mathbf{r}|^3} d^3x d^3y. \quad (2)$$

This is the flux-weighted average, over all pairs of magnetic field lines $d\mathbf{x}/ds = \mathbf{B}(\mathbf{x})$, $d\mathbf{y}/ds = \mathbf{B}(\mathbf{y})$, of the Gauss linking integral

$$L(\mathbf{x}, \mathbf{y}) = \frac{1}{4\pi} \oint_{\mathbf{x}(s)} \oint_{\mathbf{y}(s)} \frac{d\mathbf{x}}{ds} \cdot \frac{d\mathbf{y}}{ds} \times \frac{\mathbf{r}}{|\mathbf{r}|^3} ds ds'. \quad (3)$$

The Gauss integral is integer-valued and measures the net linking of a pair of closed curves (Ricca & Nipoti 2011).

Unfortunately, the gauge invariance of H relies on the condition $B_n|_{\partial V} = 0$. In astrophysical situations such as the solar atmosphere, this condition is generally violated. In a seminal paper, Berger & Field (1984) showed how gauge invariance may be restored by measuring the helicity with respect to a chosen reference magnetic field \mathbf{B}' sharing the same distribution of B_n on ∂V . This relative helicity, which we shall denote $H_{\mathbf{B}'}(\mathbf{B})$, is then an ideal invariant under motions that vanish on ∂V . It has since been widely applied to the open magnetic fields arising in solar physics (see the review by Démoulin 2007).

This work is motivated by a fundamental question: is there a topological interpretation of relative helicity in open fields analogous to the linking number interpretation of H (Equation (2)) in closed fields? Since the magnetic field lines are no longer closed curves, they no longer have invariant Gauss linking integrals. However, one can construct alternative invariants for pairs of curves stretching between two planes, provided that the end-points are held fixed (Berger 1986, 1993). Indeed, we will show in Section 4 that it is possible to express both H and $H_{\mathbf{B}'}$ in terms of these “winding numbers.” The fact that there are multiple ways of defining such invariant winding numbers reflects the fact that neither H nor $H_{\mathbf{B}'}$ is uniquely defined for an open field. Rather, H depends on the choice of gauge, and $H_{\mathbf{B}'}$ on the choice of reference field. In fact, we argue in Section 5 that H is no less meaningful than $H_{\mathbf{B}'}$ in an open field, despite the fact that the latter has been used preferentially in applications.

In solar physics, the non-uniqueness of $H_{\mathbf{B}'}$ has almost universally been circumvented by choosing \mathbf{B}' to be the unique potential field \mathbf{B}^p matching B_n on the boundary of the domain. The potential field is well-defined and has the minimum magnetic energy of all fields matching the same boundary conditions. In the case of magnetic fields rooted in a single planar boundary, $H_{\mathbf{B}^p}$ has been shown explicitly to be an average winding number (Berger 1986; Démoulin 2006). This physical interpretation has been used to infer the injection of relative helicity into the Sun’s corona by tracking the winding of magnetic field lines by their footpoint motions on the photospheric boundary (Démoulin 2007). However, there are two limitations that prevent $H_{\mathbf{B}^p}$ from being a perfect helicity measure. The first

limitation is that, if the boundary conditions $B_n|_{\partial V}$ are changing in time, then the reference field \mathbf{B}^p will itself change in time, and usually in a non-ideal way. This means that the evolution of the relative helicity will mix up both real topological changes in \mathbf{B} and those simply due to the change of \mathbf{B}^p . The second limitation is that, in a domain with more than one boundary where $B_n \neq 0$, the interpretation of $H_{\mathbf{B}^p}$ as measuring the average winding number breaks down. This is shown in Section 5. Our central idea in this paper is that these limitations may be overcome by defining helicity not through $H_{\mathbf{B}^p}$, but by fixing a special gauge in H . Fixing the gauge of H will always create an ideal invariant that is (trivially) gauge independent. Our main contribution is to show in Section 3 how this invariant is physically meaningful.

It should be mentioned that several authors have proposed other alternatives to the widely used $H_{\mathbf{B}^p}$. For example, Longcope & Malanushenko (2008) have explored different choices of reference field for relative helicity in sub-volumes of the solar corona. Low (2006) has proposed a “Lagrangian helicity” that decomposes \mathbf{B} at some initial time into a toroidal and a poloidal component, then measures the linking between the two components mapped back to the initial configuration (see also Webb et al. 2010; Low 2011). This retains a freedom in the choice of the initial toroidal–poloidal decomposition. Closer in spirit to the present paper, Hornig (2006) proposes to define H completely with a particular choice of gauge, namely $\nabla^\perp \cdot \mathbf{A} = 0$ on the boundary (where ∇^\perp denotes the component of the gradient tangential to the boundary). Jensen & Chu (1984) also imposed a gauge condition—that $\mathbf{n} \times \mathbf{A} = \mathbf{n} \times \mathbf{A}^p$ on ∂V —to uniquely define their version of relative helicity, which has the form

$$H^{\text{JC}} = \int_V \mathbf{A} \cdot \mathbf{B} d^3x - \int_V \mathbf{A}^p \cdot \mathbf{B}^p d^3x. \quad (4)$$

Such gauge conditions are also frequently used to simplify the calculation of $H_{\mathbf{B}^p}$ in practice (Démoulin 2007). For the particular case of a cylindrical domain, Low (2011) introduced an “absolute helicity” that is similarly based on fixing a particular gauge of \mathbf{A} (related to a toroidal–poloidal, or Chandrasekhar–Kendall decomposition). The geometric characterization of the helicity in any gauge which we highlight in this study allows for comparison of our fixed gauge measure with these alternatives. It is demonstrated in Section 4.2 that all choices except the one we propose in this paper measure the field-line winding in a manner which is not wholly physically meaningful.

The layout of this paper is as follows. We briefly review the standard definitions of H and of the relative helicity $H_{\mathbf{B}^p}$ in Section 2, before introducing an important special gauge in Section 3 which we call the “winding gauge.” Section 4 then presents the main contributions of this paper: (1) that H is physically meaningful in any gauge, and (2) that the winding gauge best captures our intuitive idea of field line winding. In Section 5 we investigate how the “winding” helicity relates to the relative helicity. Conclusions are summarized in Section 6.

2. PRELIMINARIES

Throughout, we shall consider magnetic fields on a domain $V \in \mathbb{R}^3$ where $V = S_z \times [0, h]$ for a set of simply connected regions $S_z \subset \mathbb{R}^2$, $z \in [0, h]$, whose boundaries ∂S_z vary continuously with z . An example is shown in Figure 1(a). Each of the foliating surfaces S_z has the same normal vector $\hat{\mathbf{z}}$. The boundary of V consists of the lower boundary surface S_0 , the

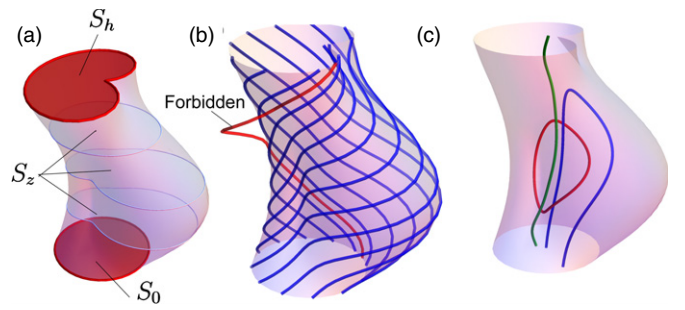


Figure 1. Domain V and its admissible magnetic field lines. Panel (a) depicts an example domain. Panel (b) shows (in blue) a set of admissible field lines which are tangent to the boundary, and a red forbidden field line that is not allowed in this paper. Panel (c) shows the three possible connectivities that an admissible field line may have.

(A color version of this figure is available in the online journal.)

upper boundary surface S_h , and the set $S_z = \{\partial S_z | z \in (0, h)\}$, i.e. $\partial V = S_0 \cup S_z \cup S_h$. We define a Cartesian co-ordinate system $\{\hat{\mathbf{e}}_1, \hat{\mathbf{e}}_2, \hat{\mathbf{z}}\}$ for V with the pair $\{\hat{\mathbf{e}}_1, \hat{\mathbf{e}}_2\}$ spanning the surfaces S_z .

We consider magnetic fields \mathbf{B} which are either tangent or zero on the side boundary S_s , but place no restrictions on the end boundaries S_0 and S_h . The conditions on S_s forbid magnetic field lines from leaving the boundary (see Figure 1(b)). If B_z has the same sign everywhere in V , then the magnetic field will essentially be a directional flow through the domain, akin to a magnetic flux rope. However, our set of admissible magnetic fields is wider and allows for a mixture of field lines linking the two end planes, field lines that are looped, and those that are closed (examples are depicted in Figure 1(c)). It also allows for fields in a half-space $h \rightarrow \infty$, $S_z = \mathbb{R}^2$, $\forall z \in [0, \infty)$. In this case a reasonable definition of helicity requires that the field decays to zero toward infinity, implying a looped field of the type discussed by Démoulin et al. (2006).

2.1. Magnetic Helicity

We shall denote the magnetic helicity by

$$H(\mathbf{B}) = \int_V \mathbf{A} \cdot \mathbf{B} d^3x. \quad (5)$$

In a magnetically open domain V , the helicity depends on the gauge of \mathbf{A} . For under a gauge transformation $\mathbf{A} \rightarrow \mathbf{A}' = \mathbf{A} + \nabla \chi$, we find

$$H \rightarrow H' = H + \oint_{\partial V} \chi B_n d^2x. \quad (6)$$

So if the normal magnetic field B_n is non-zero anywhere on the boundary ∂V , we can change H by changing the gauge χ . For our domain (described above) we have $B_n = 0$ on the side boundary S_s , so

$$H \rightarrow H' = H + \int_{S_h} \chi B_z d^2x - \int_{S_0} \chi B_z d^2x. \quad (7)$$

2.2. Relative Helicity

The original definition of relative helicity for open magnetic fields invokes an imagined extension of V to a larger volume $V \cup \tilde{V}$ (Berger & Field 1984), whose outer boundary is a magnetic surface. Examples of this extended domain are shown in Figure 2. We let $\tilde{\mathbf{B}}$ be some magnetic field on \tilde{V} such that \tilde{B}_n

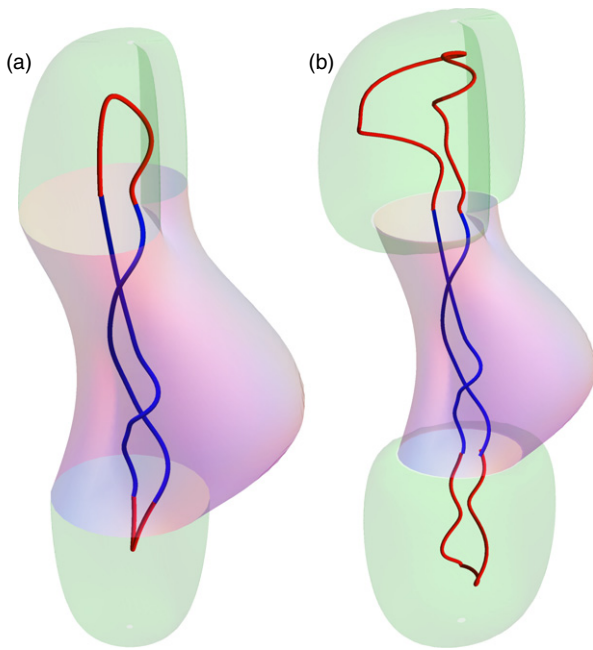


Figure 2. Extended volume $V \cup \tilde{V}$ in the original definition of relative helicity by Berger & Field (1984), for two different choices of extension \tilde{V} . Note that the field lines of $\tilde{\mathbf{B}}$ close the existing field lines.

(A color version of this figure is available in the online journal.)

matches B_n on the boundary of the original volume V , and \tilde{B}_n vanishes on the outer boundary of the combined volume. Let

$$H(\mathbf{B}, \tilde{\mathbf{B}}) := \int_V \mathbf{A} \cdot \mathbf{B} d^3x + \int_{\tilde{V}} \tilde{\mathbf{A}} \cdot \tilde{\mathbf{B}} d^3x, \quad \text{where } \tilde{\mathbf{B}} = \nabla \times \tilde{\mathbf{A}}. \quad (8)$$

Then the *relative helicity* of \mathbf{B} with respect to reference field \mathbf{B}' on V is defined as

$$H_{\mathbf{B}'}(\mathbf{B}) := H(\mathbf{B}, \tilde{\mathbf{B}}) - H(\mathbf{B}', \tilde{\mathbf{B}}), \quad (9)$$

for any choice $\tilde{\mathbf{B}}$ of extension field, where \mathbf{B}' must satisfy the boundary condition $B'_n|_{\partial V} = B_n|_{\partial V}$.

We can show that the relative helicity $H_{\mathbf{B}'}(\mathbf{B})$ is independent of the choice of extension $\tilde{\mathbf{B}}$, and depends neither on the gauge of \mathbf{A} nor on that of \mathbf{A}' . To ensure continuity of the vector potential in $H(\mathbf{B}, \tilde{\mathbf{B}})$ and $H(\mathbf{B}', \tilde{\mathbf{B}})$, we must use different vector potentials for $\tilde{\mathbf{B}}$ in each case. If we choose $\mathbf{n} \times \tilde{\mathbf{A}}|_{\partial V} = \mathbf{n} \times \mathbf{A}|_{\partial V}$ for the first case, then we have $\mathbf{n} \times \tilde{\mathbf{A}}' = \mathbf{n} \times \mathbf{A} + \mathbf{n} \times \nabla \psi$ for the second case. So

$$\begin{aligned} H_{\mathbf{B}'}(\mathbf{B}) &= \int_V (\mathbf{A} \cdot \mathbf{B} - \mathbf{A}' \cdot \mathbf{B}') d^3x - \int_{\tilde{V}} \nabla \psi \cdot \tilde{\mathbf{B}} d^3x, \\ &= \int_V (\mathbf{A} \cdot \mathbf{B} - \mathbf{A}' \cdot \mathbf{B}') d^3x + \oint_{\partial V} \psi B_n d^2x. \end{aligned}$$

Now

$$\int_V (\mathbf{A}' \cdot \mathbf{B} - \mathbf{A} \cdot \mathbf{B}') d^3x = \int_V (\mathbf{A}' \cdot \nabla \times \mathbf{A} - \mathbf{A} \cdot \nabla \times \mathbf{A}') d^3x, \quad (10)$$

$$= \oint_{\partial V} \mathbf{A} \times \mathbf{A}' \cdot \mathbf{n} d^2x, \quad (11)$$

$$= \oint_{\partial V} \mathbf{A} \times (\mathbf{A}' - \mathbf{A}) \cdot \mathbf{n} d^2x, \quad (12)$$

$$= \oint_{\partial V} \mathbf{A} \times \nabla \psi \cdot \mathbf{n} d^2x, \quad (13)$$

$$= \oint_{\partial V} (\psi \nabla \times \mathbf{A} - \nabla \times (\psi \mathbf{A})) \cdot \mathbf{n} d^2x, \quad (14)$$

$$= \oint_{\partial V} \psi B_n d^2x. \quad (15)$$

The last line follows from Stokes' Theorem since ∂V is a closed surface. Hence

$$H_{\mathbf{B}'}(\mathbf{B}) = \int_V (\mathbf{A} + \mathbf{A}') \cdot (\mathbf{B} - \mathbf{B}') d^3x. \quad (16)$$

This is often known as the Finn & Antonsen (1985) formula for relative helicity. Since $\tilde{\mathbf{B}}$ appears nowhere in (16), we see that $H_{\mathbf{B}'}(\mathbf{B})$ is independent of the extension $\tilde{\mathbf{B}}$. Gauge invariance readily follows from this formula, for if either $\mathbf{A} \rightarrow \mathbf{A} + \nabla \chi$ or $\mathbf{A}' \rightarrow \mathbf{A}' + \nabla \chi$, then

$$H_{\mathbf{B}'}(\mathbf{B}) \rightarrow H_{\mathbf{B}'}(\mathbf{B}) + \oint_{\partial V} \chi (B_n - B'_n) d^2x, \quad (17)$$

and the last integral vanishes by the boundary condition on \mathbf{B}' .

The main limitation of the relative helicity is that it depends on the choice of reference field \mathbf{B}' , and this complicates its physical interpretation. We return to address this point in Section 5.

3. THE WINDING GAUGE

In Section 4, we will show that H for an open magnetic field in a domain V such as we consider may be interpreted as an average winding number, analogous to the interpretation of H for a closed magnetic field as an average linking integral. Central to this interpretation will be a specific choice of gauge for \mathbf{A} that is analogous to the Coulomb gauge of Equation (1). The difference in the open case is that the choice of gauge will now affect the value of H , not just its integral expression. Nevertheless, this specific gauge—which we call “winding”—will turn out to be physically meaningful.

For an open field, we cannot use the Coulomb gauge (1) since it will generally violate $\nabla \times \mathbf{A} = \mathbf{B}$ when $B_n|_{\partial V} \neq 0$. However, since $B_n = 0$ on the side boundary of our cylinder V , it is possible to use a two-dimensional equivalent of the Coulomb gauge whose horizontal divergence $\nabla^\perp \cdot \mathbf{A} = 0$ vanishes (but not its full three-dimensional divergence). This is what we call the *winding gauge*, and may be written

$$\mathbf{A}^W(x_1, x_2, z) = \frac{1}{2\pi} \int_{S_z} \frac{\mathbf{B}(y_1, y_2, z) \times \mathbf{r}}{|\mathbf{r}|^2} d^2y, \quad (18)$$

where $\mathbf{r} = (x_1 - y_1, x_2 - y_2, 0)$.

In this gauge, the vector potential at any point is defined as an average over the horizontal surface S_z at that height (Figure 3).

Since we have been unable to find it in print, we include here a proof that $\nabla \times \mathbf{A}^W = \mathbf{B}$ for a magnetic field on our domain V with $B_n = 0$ on the side boundary. This is similar to the familiar proof for the three-dimensional Coulomb gauge (e.g., Cantarella et al. 2001), but there are some complications.

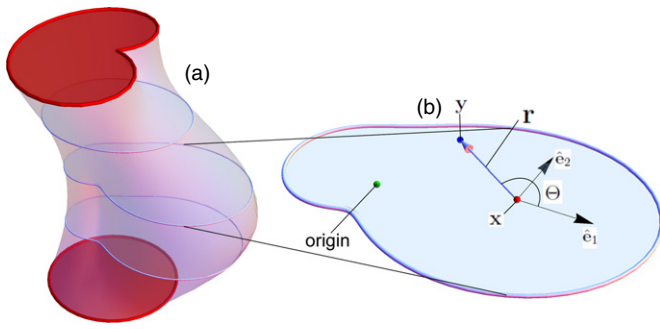


Figure 3. Vector \mathbf{r} used to define the winding gauge and measure the winding of magnetic field lines. The vector potential \mathbf{A}^W at a point on the cross-section S_z (depicted in panel b) is defined by integrating over the cross-section. Also shown is the angle Θ made by \mathbf{r} and the $\hat{\mathbf{e}}_1$ axis, and used to define the winding number.

(A color version of this figure is available in the online journal.)

First, one may show by direct differentiation that

$$\frac{\mathbf{r}}{|\mathbf{r}|^2} = \nabla_x^\perp (\log |\mathbf{r}|), \quad (19)$$

where $\nabla_x^\perp := (\partial/\partial x_1, \partial/\partial x_2, 0)$. The subscript x indicates differentiation with respect to x , as opposed to y . Thus

$$\mathbf{A}^W(\mathbf{x}) = \frac{1}{2\pi} \int_{S_z} \mathbf{B}(\mathbf{y}) \times \nabla_x^\perp (\log |\mathbf{r}|) d^2y \quad (20)$$

$$= -\frac{1}{2\pi} \nabla_x^\perp \times \left(\int_{S_z} \mathbf{B}(\mathbf{y}) \log |\mathbf{r}| d^2y \right). \quad (21)$$

To take the ∇_x^\perp operator outside the integral, we have used the fact that the geometries of the cross-sections S_z vary only as a function of the z -coordinate.

By writing out the components explicitly, one can verify for a function $\mathbf{f} = (f_1, f_2, f_3)$ that

$$\nabla \times \nabla^\perp \times \mathbf{f} = -(\nabla^\perp)^2 \mathbf{f} + \nabla^\perp (\nabla \cdot \mathbf{f}), \quad (22)$$

where ∇ is the full (three-component) operator, and

$$(\nabla^\perp)^2 \mathbf{f} = \left(\frac{\partial^2 f_1}{\partial x_1^2} + \frac{\partial^2 f_1}{\partial x_2^2}, \frac{\partial^2 f_2}{\partial x_1^2} + \frac{\partial^2 f_2}{\partial x_2^2}, \frac{\partial^2 f_3}{\partial x_1^2} + \frac{\partial^2 f_3}{\partial x_2^2} \right). \quad (23)$$

Applying this to Equation (21), we can take the derivatives inside the integral, but for the three-component operator ∇_x we must account for the fact that the shape of S_z may vary in z . Leibniz' rule adds an extra term depending on $\mathbf{v} \cdot \mathbf{n}$, where $\mathbf{v}(\mathbf{y}) = d\mathbf{y}/dz$ is a “velocity” describing how the boundary S_z changes shape in z . Since \mathbf{B} is tangent to S_z , we can simply take $\mathbf{v} = \mathbf{B}/B_z$. Applying (22) with Leibniz' rule then gives

$$\begin{aligned} \nabla_x \times \mathbf{A}^W(\mathbf{x}) &= \frac{1}{2\pi} \int_{S_z} \mathbf{B}(\mathbf{y}) (\nabla_x^\perp)^2 (\log |\mathbf{r}|) d^2y \\ &\quad - \frac{1}{2\pi} \nabla_x^\perp \times \left(\int_{S_z} \nabla_x \cdot (\mathbf{B}(\mathbf{y}) \log |\mathbf{r}|) d^2y \right) \\ &\quad + \frac{1}{2\pi} \nabla_x^\perp \oint_{\partial S_z} B_n(\mathbf{y}) \log |\mathbf{r}| dl_y. \end{aligned} \quad (24)$$

For the second term, note that

$$\nabla_x \cdot (\mathbf{B}(\mathbf{y}) \log |\mathbf{r}|) = \mathbf{B}(\mathbf{y}) \cdot \nabla_x (\log |\mathbf{r}|) + (\log |\mathbf{r}|) \nabla_x \cdot \mathbf{B}(\mathbf{y}), \quad (25)$$

$$= -\mathbf{B}(\mathbf{y}) \cdot \nabla_y (\log |\mathbf{r}|) + (\log |\mathbf{r}|) \frac{\partial B_z(\mathbf{y})}{\partial z}, \quad (26)$$

$$= -\mathbf{B}(\mathbf{y}) \cdot \nabla_y^\perp (\log |\mathbf{r}|) - (\log |\mathbf{r}|) \nabla_y^\perp \cdot \mathbf{B}(\mathbf{y}), \quad (27)$$

$$= -\nabla_y^\perp \cdot (\mathbf{B}(\mathbf{y}) \log |\mathbf{r}|). \quad (28)$$

The resulting term becomes a boundary integral and the sum of the second and third terms of (24) cancel, leaving just the first term. It may be shown that

$$(\nabla_x^\perp)^2 (\log |\mathbf{r}|) = 2\pi \delta(\mathbf{r}), \quad (29)$$

where $\delta(\mathbf{r})$ is the two-dimensional Dirac δ -function and $(\nabla_x^\perp)^2$ is the two-dimensional Laplacian. (This is a direct analogue of a widely used result in three dimensions.) It follows that $\nabla_x \times \mathbf{A}^W(\mathbf{x}) = \mathbf{B}(\mathbf{x})$ so that (18) is a valid vector potential.

4. WINDING NUMBER INTERPRETATION OF HELICITY

For a pair of field lines $\mathbf{x}(s)$, $\mathbf{y}(t)$ that are not closed within V , the Gauss linking number is not a topological invariant. Instead, we shall define the *winding number* $\mathcal{L}(\mathbf{x}, \mathbf{y})$ between two field lines in z .

First, consider the case where the z -coordinates of both field lines are monotonically increasing, as in Figure 4(a). In this case, we can parameterize both field lines by their z -coordinate. We define \mathcal{L} to be the net rotation of the vector \mathbf{r} between \mathbf{x} and \mathbf{y} as z increases from 0 to h , so

$$\begin{aligned} \mathcal{L}(\mathbf{x}, \mathbf{y}) &:= \frac{1}{2\pi} \int_0^h \frac{d}{dz} \Theta(\mathbf{x}(z), \mathbf{y}(z)) dz, \\ \text{where } \Theta(\mathbf{x}, \mathbf{y}) &= \arctan \left(\frac{x_2 - y_2}{x_1 - y_1} \right). \end{aligned} \quad (30)$$

As Θ is a multi-valued function, the boundary values on S_0 and S_h define \mathcal{L} only up to an integer, *i.e.*,

$$\mathcal{L}(\mathbf{x}, \mathbf{y}) = \frac{1}{2\pi} (\Theta(\mathbf{x}(h), \mathbf{y}(h)) - \Theta(\mathbf{x}(0), \mathbf{y}(0))) + N, \quad (31)$$

where N is the integer number of full windings of the joining vector $\mathbf{r} = \mathbf{y} - \mathbf{x}$. If the end angles remain fixed, and the field lines remain monotonic in z , the winding number is invariant to deformations of the field lines which forbid their crossing (Berger 1993; Berger & Prior 2006).

In general, the field lines \mathbf{x} and \mathbf{y} may have respectively n and m distinct points in z where they turn back on themselves, that is $dx_z/dz = 0$ or $dy_z/dz = 0$. We split \mathbf{x} into $n+1$ sections at these turning points and similarly split \mathbf{y} into $m+1$ sections. For example the blue field line in Figure 4(b) has two such turning points, so is split into three sections. Sections \mathbf{x}_i and \mathbf{y}_j share a mutual z -range $[z_{ij}^{\min}, z_{ij}^{\max}]$ (which could be an empty set), and for each of these ranges we can define an angle $\Theta(\mathbf{x}_i, \mathbf{y}_j)$ for each vector \mathbf{r}_{ij} . For example, there are three such vectors between the blue and red curves in Figure 4(c), because the blue

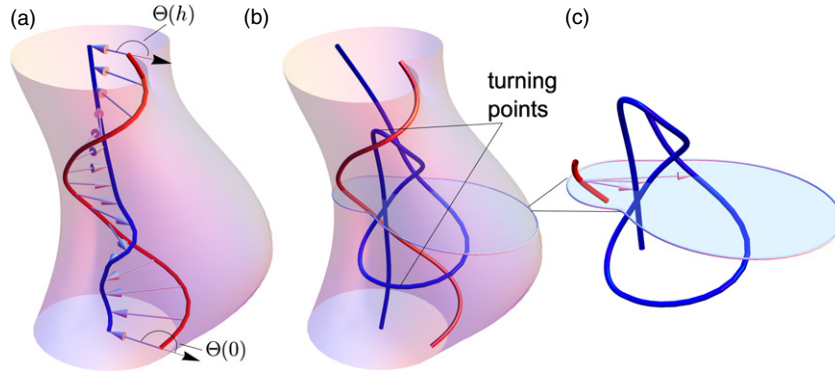


Figure 4. Geometrical interpretation of the winding number. Panel (a) depicts a pair of curves whose z -components are monotonic in z . The vectors $\mathbf{r}(z)$ joining the two curves are shown, along with the angle Θ between \mathbf{r} and the x -axis at either end. Panel (b) depicts a pair of curves for which we need to define multiple angles Θ_{ij} , owing to the fact that one curve is not monotonic in z . Panel (c) depicts an example cross-section from Panel (b), showing three vectors \mathbf{r}_{1j} , $j = 1, 2, 3$ defining angles on a particular plane S_z .

(A color version of this figure is available in the online journal.)

curve has three sections passing through this plane. Berger & Prior (2006) defined the sum

$$\mathcal{L}(\mathbf{x}, \mathbf{y}) := \sum_{i=1}^{n+1} \sum_{j=1}^{m+1} \frac{\sigma(\mathbf{x}_i) \sigma(\mathbf{y}_j)}{2\pi} \int_{z_{ij}^{\min}}^{z_{ij}^{\max}} \frac{d\Theta(\mathbf{x}_i(z), \mathbf{y}_j(z))}{dz} dz. \quad (32)$$

where $\sigma(\mathbf{x}_i)$ is an indicator function marking whether the curve section \mathbf{x}_i moves up or down in z ; for example,

$$\sigma(\mathbf{x}_i) = \begin{cases} 1 & \text{if } dx_z/dz > 0, \\ -1 & \text{if } dx_z/dz < 0. \end{cases} \quad (33)$$

It was shown that under this extended definition that $\mathcal{L}(\mathbf{x}, \mathbf{y})$ remains invariant to all deformations which vanish at the bounding planes S_0 , S_h and forbid self-crossings. Importantly, this remains true whether one or both field lines are anchored only at one plane, or are closed in V (Berger & Prior 2006). For example, it could be applied to any pair of curves in Figure 1(c). It was further shown that for closed curves \mathcal{L} has the same integer value as the Gauss linking integral (3). We re-iterate that the winding number is not equal to the Gauss linking integral for open curves. Indeed, the linking number is not an invariant in such cases, so the winding number framework for topological classification is applicable to a much larger set of admissible magnetic fields.

4.1. Winding Gauge

Our goal in this section is to express H as an average pairwise winding between the field lines that make up the open magnetic field. First, we will show this for the winding gauge of Section 3, then we will consider what happens in a general gauge.

If \mathbf{A} is written in the winding gauge (18), we will show that the corresponding helicity H , which we shall denote H^W , is related to the winding numbers by

$$\begin{aligned} H^W(\mathbf{B}) &:= \int_V \mathbf{A}^W \cdot \mathbf{B} d^3x \\ &= \frac{1}{2\pi} \int_0^h \int_{S_z \times S_z} \frac{d}{dz} \Theta(\mathbf{x}, \mathbf{y}) B_z(\mathbf{x}) B_z(\mathbf{y}) d^2x d^2y dz. \end{aligned} \quad (34)$$

So the helicity is the average pairwise winding between all local portions of field lines. To relate H^W to the winding of entire field

lines, consider the flux-weighted winding number

$$\mathcal{L}_B(\mathbf{x}, \mathbf{y}) := \sum_{i=1}^{n+1} \sum_{j=1}^{m+1} \frac{1}{2\pi} \int_{z_{ij}^{\min}}^{z_{ij}^{\max}} \frac{d\Theta(\mathbf{x}_i(z), \mathbf{y}_j(z))}{dz} \times B_z(\mathbf{x}_i) B_z(\mathbf{y}_j) dz. \quad (35)$$

Like \mathcal{L} , this is invariant under deformations that vanish on S_0 , S_h and forbid self-crossings. (The B_z functions have the same sign as the σ functions in (32).) Then H^W may be formally written as the average flux-weighted winding number over all pairs of field lines $\mathbf{x}(s)$, $\mathbf{y}(s)$, or

$$H^W(\mathbf{B}) = \int \mathcal{L}_B(\mathbf{x}, \mathbf{y}) d\mathbf{x} d\mathbf{y}. \quad (36)$$

In the particular case where the z -coordinates of all field lines are monotonically increasing, H^W may be written as an integral of the original winding number $\mathcal{L}(\mathbf{x}, \mathbf{y})$ over S_0 ,

$$H^W(\mathbf{B}) = \int_{S_0} \mathcal{L}(\mathbf{x}, \mathbf{y}) B_z(\mathbf{x}) B_z(\mathbf{y}) d^2x d^2y. \quad (37)$$

In this case, one can also write

$$H^W(\mathbf{B}) = \int_{S_0} \mathcal{A}^W(\mathbf{x}) B_z(\mathbf{x}) d^2x, \quad (38)$$

where the *flux function*

$$\mathcal{A}^W(\mathbf{x}) := \int_{\mathbf{x}(z)} \frac{\mathbf{A}^W \cdot \mathbf{B}}{|B_z|} dz \quad (39)$$

is obtained by integrating the vector potential over a particular field line $\mathbf{x}(z)$. Although we do not dwell on it in this paper, notice that the flux function \mathcal{A}^W is also a physically meaningful ideal invariant. In fact for fields with $B_z > 0$ everywhere it has been shown to be more powerful than the helicity H^W and able to distinguish between topologically different magnetic fields with the same H^W (Yeates & Hornig 2013).

To prove Equation (34), consider the helicity density

$$\mathbf{A}^W \cdot \mathbf{B} = \mathbf{B}(\mathbf{x}) \cdot \left(\frac{1}{2\pi} \int_{S_z} \frac{\mathbf{B}(\mathbf{y}) \times \mathbf{r}}{|\mathbf{r}|^2} d^2y \right), \quad (40)$$

$$= \frac{1}{2\pi} \left(\mathbf{B}^\perp(\mathbf{x}) \cdot \int_{S_z} B_z(\mathbf{y}) \frac{\hat{\mathbf{z}} \times \mathbf{r}}{|\mathbf{r}|^2} d^2y - B_z(\mathbf{x}) \int_{S_z} \mathbf{B}^\perp(\mathbf{y}) \cdot \frac{\hat{\mathbf{z}} \times \mathbf{r}}{|\mathbf{r}|^2} d^2y \right), \quad (41)$$

$$= \frac{1}{2\pi} \int_{S_z} \left(\frac{\mathbf{B}^\perp(\mathbf{x})}{B_z(\mathbf{x})} - \frac{\mathbf{B}^\perp(\mathbf{y})}{B_z(\mathbf{y})} \right) \cdot \frac{\hat{\mathbf{z}} \times \mathbf{r}}{|\mathbf{r}|^2} B_z(\mathbf{y}) B_z(\mathbf{x}) d^2y. \quad (42)$$

Now, differentiating $\Theta(\mathbf{x}, \mathbf{y})$ with respect to z yields

$$\frac{d}{dz} \Theta(\mathbf{x}(z), \mathbf{y}(z)) = \frac{r_1^2}{|\mathbf{r}|^2} \frac{d}{dz} \left(\frac{r_2}{r_1} \right), \quad (43)$$

$$= \frac{1}{|\mathbf{r}|^2} \left(r_1 \frac{dr_2}{dz} - r_2 \frac{dr_1}{dz} \right), \quad (44)$$

$$= \frac{1}{|\mathbf{r}|^2} \left\{ r_1 \left(\frac{B_2(\mathbf{x})}{B_z(\mathbf{x})} - \frac{B_2(\mathbf{y})}{B_z(\mathbf{y})} \right) - r_2 \left(\frac{B_1(\mathbf{x})}{B_z(\mathbf{x})} - \frac{B_1(\mathbf{y})}{B_z(\mathbf{y})} \right) \right\}. \quad (45)$$

Here we have used that $\mathbf{x}(z), \mathbf{y}(z)$ are segments of magnetic field lines. Since $\hat{\mathbf{z}} \times \mathbf{r} = (-r_2, r_1, 0)$, we arrive at

$$\mathbf{A}^W \cdot \mathbf{B} = \frac{1}{2\pi} \int_{S_z} \frac{d}{dz} \Theta(\mathbf{x}, \mathbf{y}) B_z(\mathbf{y}) B_z(\mathbf{x}) d^2y, \quad (46)$$

and integrating over V gives Equation (34).

It is important to notice that Equation (34) defines $H^W(\mathbf{B})$ uniquely using only \mathbf{B} itself, without reference to \mathbf{A} . This reinforces the fact that H^W is a physically meaningful quantity, despite the absence of an explicit reference field. The interpretation of H^W as an average pairwise winding number is analogous to the interpretation of H for a closed field as a flux-weighted average of the linking number between all pairs of field lines. The fact that the winding number $\mathcal{L}(\mathbf{x}, \mathbf{y})$ of a closed curve is equal to the linking number (3) mirrors the fact that, for a closed field, H^W matches the value of H obtained with the Coulomb gauge (1), owing to the gauge independence of H for closed fields.

One last note in this section is the fact that the winding number expression (34) for the topology of open fields was obtained by Berger (1986) for a field in the half space (decaying at a sufficient rate toward infinity). In that case it was attributed to the *relative helicity* $H_{\mathbf{B}^p}(\mathbf{B})$ with a potential reference field \mathbf{B}^p . As we shall see in Section 5.2.2, the identification of $H_{\mathbf{B}^p}(\mathbf{B})$ with average winding is not always true for the more general set of fields we consider here, whilst we have seen that H^W always has this interpretation.

4.2. Other Gauges

What is the physical meaning of H in a gauge other than the winding gauge? In such a gauge we have $\mathbf{A}' = \mathbf{A}^W + \nabla \chi$ for some scalar function χ . It turns out that the choice of χ corresponds to a particular choice of *frame field* for defining the angle Θ .

In (30), we defined Θ as $\arctan(r_2/r_1)$, where r_1, r_2 are the components of \mathbf{r} with respect to a particular orthonormal

Cartesian frame $\{\hat{\mathbf{e}}_1, \hat{\mathbf{e}}_2\}$. But suppose we choose a different orthonormal frame $\{\hat{\mathbf{e}}'_1, \hat{\mathbf{e}}'_2\}$, rotated through angle θ with respect to $\{\hat{\mathbf{e}}_1, \hat{\mathbf{e}}_2\}$. Then the components of \mathbf{r} with respect to the new frame are

$$r'_1 = r_1 \cos \theta - r_2 \sin \theta, \quad r'_2 = r_1 \sin \theta + r_2 \cos \theta. \quad (47)$$

Defining the angle with respect to this new frame gives a different result

$$\Theta' := \arctan \left(\frac{r'_2}{r'_1} \right) = \arctan \left(\frac{r_2/r_1 + \tan \theta}{1 - (r_2/r_1) \tan \theta} \right) = \Theta + \theta. \quad (48)$$

On a particular cross section S_z , the new winding rate relates to the old winding rate through

$$\frac{d}{dz} \Theta'(\mathbf{x}, \mathbf{y}) = \frac{d}{dz} \Theta(\mathbf{x}, \mathbf{y}) + \frac{d}{dz} \theta(\mathbf{x}), \quad (49)$$

and the new winding number of the curves \mathbf{x} and \mathbf{y} is

$$\begin{aligned} \mathcal{L}'_{\mathbf{B}}(\mathbf{x}, \mathbf{y}) &= \mathcal{L}_{\mathbf{B}}(\mathbf{x}, \mathbf{y}) + \sum_{i=1}^{n+1} \sum_{j=1}^{m+1} \frac{1}{2\pi} \\ &\times \int_{z_i^{\min}}^{z_i^{\max}} \frac{d}{dz} \theta(\mathbf{x}_i) B_z(\mathbf{x}_i) B_z(\mathbf{y}_j) dz. \end{aligned} \quad (50)$$

This reduces to $\mathcal{L}_{\mathbf{B}}(\mathbf{x}, \mathbf{y})$ if θ is constant (i.e., if we always measure Θ with respect to the same frame). However, if there is a net change in θ along the field line $\mathbf{x}(z)$, then the new winding number $\mathcal{L}'_{\mathbf{B}}(\mathbf{x}, \mathbf{y})$ differs from the old $\mathcal{L}_{\mathbf{B}}(\mathbf{x}, \mathbf{y})$. It should be pointed out that the new winding measure remains invariant to ideal motions, but now part of its value is due to a non-physical quantity: the rotation of the frame field. An example will be shown in Section 4.3.

To see that our frame field corresponds to a change of gauge, we can substitute (49) into (34) to find that

$$\begin{aligned} &\frac{1}{2\pi} \int_0^h \int_{S_z \times S_z} \frac{d}{dz} \Theta'(\mathbf{x}, \mathbf{y}) B_z(\mathbf{x}) B_z(\mathbf{y}) d^2x d^2y dz \\ &= H^W(\mathbf{B}) + \frac{\Phi_0}{2\pi} \int_0^h \int_{S_z} \frac{d}{dz} \theta(\mathbf{x}) B_z(\mathbf{x}) d^2x dz. \end{aligned} \quad (51)$$

Using Equation (7), and if the gauge function χ satisfies

$$\int_{S_h} \chi B_z d^2x - \int_{S_0} \chi B_z d^2x = \frac{\Phi_0}{2\pi} \int_0^h \int_{S_z} \frac{d\theta}{dz} B_z d^2x dz, \quad (52)$$

it follows that

$$H'(\mathbf{B}) = \frac{1}{2\pi} \int_0^h \int_{S_z \times S_z} \frac{d}{dz} \Theta'(\mathbf{x}, \mathbf{y}) B_z(\mathbf{x}) B_z(\mathbf{y}) d^2x d^2y dz. \quad (53)$$

For example, given the frame field $\theta(\mathbf{x})$, one could take the gauge function

$$\chi(x_1, x_2, z) = \frac{z}{2\pi h} \int_{S_z} \frac{d}{dz} \theta(\mathbf{y}) B_z(\mathbf{y}) d^2y dz, \quad (54)$$

but there are many possible gauges that will give the same helicity as a particular frame field.

In summary, Equation (53) shows that the helicity in an arbitrary gauge is still the average pairwise winding number,

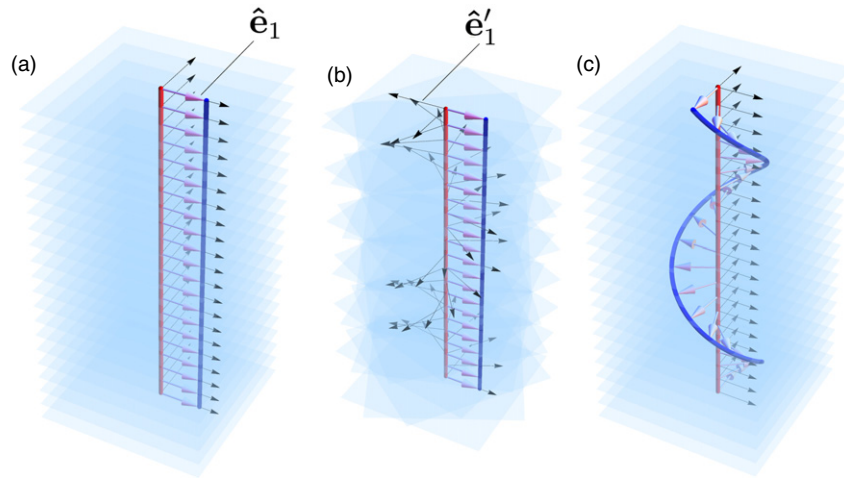


Figure 5. How a straight field can appear twisted when measured with respect to a rotating frame. Panel (a) depicts a pair of straight field lines (from a field $\mathbf{B} = \hat{\mathbf{z}}$) and their joining vectors $\mathbf{r}(z)$, which have no winding. Panel (b) shows the same figure with a varying basis indicated by the black rotating arrows. The angle between \mathbf{r} and $\hat{\mathbf{e}}'_1$ in this basis would rotate with z . Panel (c) shows two field lines of a helical field $\mathbf{B} = \hat{\mathbf{z}} + (3\pi/R_0)r\mathbf{e}_\phi$, one of which is straight (at $r = 0$). The pairwise winding of these two field lines in the original basis is the same as that of the straight field in the rotated basis.

(A color version of this figure is available in the online journal.)

but now the winding number is measured with respect to a frame field $\theta(\mathbf{x})$ that varies in space. In most situations, it seems more physically meaningful to measure winding with respect to a fixed frame, in which case the winding gauge is most appropriate. A different choice of gauge corresponds to measuring winding with respect to a varying frame, whereby even a straight magnetic field may appear tangled. This is highlighted in the following example.

4.3. Example

To illustrate the idea of Section 4.2, consider the uniform vertical field $\mathbf{B} = \hat{\mathbf{z}}$, in a circular cylinder of radius R_0 and height h . One may show by direct calculation from (18) that the winding-gauge vector potential of this field is $\mathbf{A}^W(r, \phi, z) = (r/2)\hat{\mathbf{e}}_\phi$ in standard cylindrical coordinates, and hence that $H^W(\mathbf{B}) = 0$. This is consistent with the fact that all field lines of \mathbf{B} are vertical and untwisted, so that all pairwise winding numbers $\mathcal{L}(\mathbf{x}, \mathbf{y})$ vanish when measured with respect to a fixed frame (Figure 5(a)).

However, suppose that we measure the winding numbers with respect to a frame field $\theta(z)$ that varies in z but (for simplicity) not in r, ϕ . Then each pair of field lines have the same non-zero winding number

$$\mathcal{L}'(\mathbf{x}, \mathbf{y}) = \mathcal{L}_0 := \frac{1}{2\pi} \int_0^h \frac{d}{dz} \theta(z) dz, \quad (55)$$

proportional to the net rotation of the frame. According to Section 4.2, this corresponds to measuring H with the vector potential $\mathbf{A}^W + \nabla\chi$, where

$$\chi(z) = \frac{z}{2\pi h} \int_{S_z} \int \frac{d}{dz} \theta(z) B_z d^2x dz = \frac{\pi R_0^2 z}{h} \mathcal{L}_0. \quad (56)$$

In this new gauge, $H(\mathbf{B})$ will take the non-zero value $H'(\mathbf{B}) = (\pi R_0^2)^2 \mathcal{L}_0$. For example, in Figure 5(b) we have chosen to rotate the frame by $\theta(z) = 3\pi z$ (hence if $h = 1$, $\mathcal{L}_0 = 3/2$). In fact, this is exactly the helicity one would get using the winding gauge but for a uniformly twisted magnetic field $\mathbf{B} = \hat{\mathbf{z}} + (2\pi \mathcal{L}_0/R_0)r\hat{\mathbf{e}}_\phi$ (cf. the calculation in Appendix A), whose field lines are helices, as depicted in Figure 5(c).

In other words, by defining winding with respect to a twisted frame field θ , our straight magnetic field appears twisted. If we choose an arbitrary gauge to define H , we are effectively changing our definition of “untwisted.” The winding gauge is the natural choice because then H^W is measuring the net winding with respect to a straight field. We feel that this is an important issue to highlight as it provides a geometrical insight into the meaning of the choice of gauge, and consequently a clear reason for showing preference to a particular gauge. If one were asked to measure the winding of a pair of field lines, it would be unnatural to measure the angle made by the two curves Θ with respect to anything but a fixed frame; yet, as we shall see in the following section, defining the relative helicity with a potential reference field is in many cases equivalent to choosing a varying frame whose net rotation is non-zero.

5. COMPARISON WITH RELATIVE HELICITY

We have shown that the magnetic helicity H of an open magnetic field may be physically interpreted as an average winding. Changing the gauge reflects a change in how the winding numbers are measured, but there is a unique gauge that measures winding with respect to a fixed frame: the winding gauge introduced in Section 3. In this section, we compare the corresponding helicity H^W with the relative helicity $H_{\mathbf{B}'}$ that is typically used in solar physics. This comparison helps us to address the question of whether the potential field \mathbf{B}^p is “untwisted” (in the sense of $H^W(\mathbf{B}^p) = 0$), and leads to a proof of the “equivalence” of standard and relative helicity.

5.1. General relation

Let $H^W(\mathbf{B})$ denote the winding helicity of \mathbf{B} as defined in Equation (34), and let $H_{\mathbf{B}'}(\mathbf{B})$ be the relative helicity with some reference field \mathbf{B}' . Then we claim that

$$H_{\mathbf{B}'}(\mathbf{B}) = H^W(\mathbf{B}) - H^W(\mathbf{B}'). \quad (57)$$

In other words, the cross term in Equation (16) vanishes if both \mathbf{A} and \mathbf{A}' are written in winding gauge. Note that the winding gauge is not the only gauge for which the cross-term in (16) vanishes; for example, this property is shared by the cylindrical

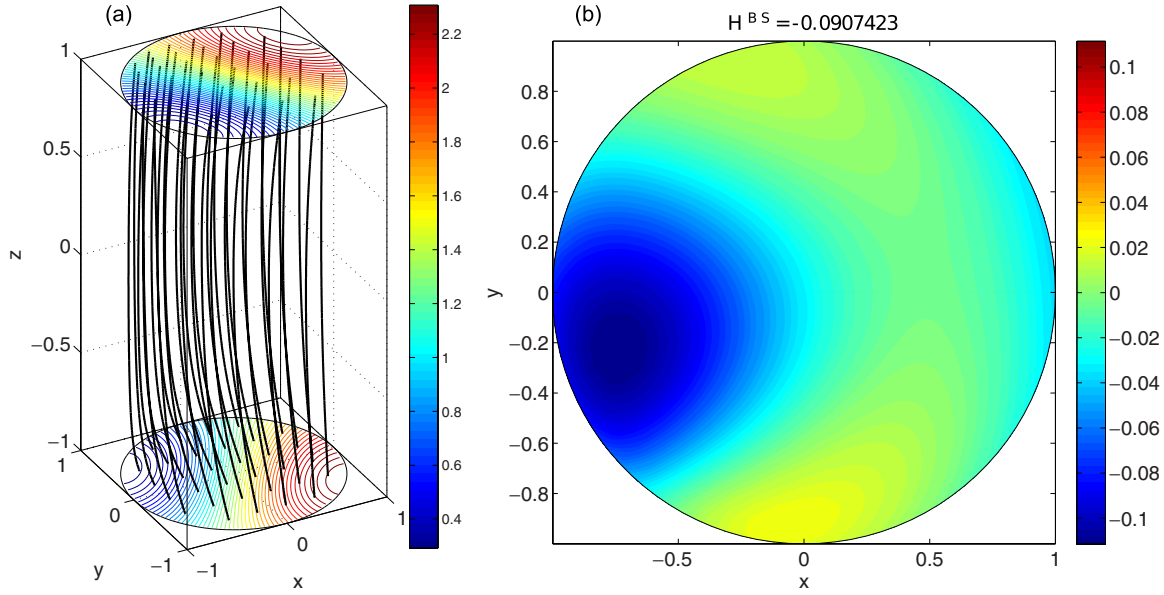


Figure 6. Potential field with $H^W \neq 0$, as described in Section 5.2.2. Panel (a) shows magnetic field lines and contours of B_z on S_0 and S_h . Panel (b) shows contours of A^W on S_0 (color shading), which integrate (weighted by B_z) to give a negative net H^W .

(A color version of this figure is available in the online journal.)

helicity of Low (2011) and the gauge choice of Valori et al. (2012). To prove (57) for the winding gauge, note that

$$\int_V \mathbf{A}' \cdot \mathbf{B} d^3x = \frac{1}{2\pi} \int_0^h \int_{S_z \times S_z} \mathbf{B}(\mathbf{x}) \cdot \frac{\mathbf{B}'(\mathbf{y}) \times \mathbf{r}}{|\mathbf{r}|^2} d^2y d^2x dz, \quad (58)$$

$$= -\frac{1}{2\pi} \int_0^h \int_{S_z \times S_z} \mathbf{B}'(\mathbf{y}) \cdot \frac{\mathbf{B}(\mathbf{x}) \times \mathbf{r}}{|\mathbf{r}|^2} d^2y d^2x dz, \quad (59)$$

$$= \frac{1}{2\pi} \int_0^h \int_{S_z \times S_z} \mathbf{B}'(\mathbf{x}) \cdot \frac{\mathbf{B}(\mathbf{y}) \times \mathbf{r}}{|\mathbf{r}|^2} d^2y d^2x dz, \quad (60)$$

$$= \int_V \mathbf{A} \cdot \mathbf{B}' d^3x. \quad (61)$$

Of course, the choice of winding gauge for either \mathbf{A} or \mathbf{A}' does not change the value of the relative helicity: only the choice of reference field \mathbf{B}' does this. It is clear from (57) that choosing a reference field with vanishing $H^W(\mathbf{B}')$ will make the relative helicity equal to $H^W(\mathbf{B})$, so that it inherits the same physical meaning.

5.2. Untwisted Reference Fields

A magnetic field with $H^W(\mathbf{B}) = 0$ might be described as “untwisted” in a well-defined physical sense. If we use such a field as the reference field in the relative helicity, then Equation (57) shows that the relative helicity reduces to H^W . It is therefore interesting to find that the most commonly used reference field—the potential field in V —does not always satisfy $H^W(\mathbf{B}) = 0$. In this section we assume (for concreteness) that V is a circular cylinder $\{0 \leq r \leq R_0, 0 \leq \phi < 2\pi, -L \leq z \leq L\}$. For consistency, we continue to denote the lower and upper boundaries by S_0 and S_h , and the side boundary by S_s .

5.2.1. Periodic Boundary Conditions

For a *periodic* magnetic field, i.e., when $B_z(r, \phi, L) = B_z(r, \phi, -L)$, a simple choice of reference field with $H^W(\mathbf{B}') = 0$ is the vertical field $\mathbf{B}'(r, \phi, z) = B_z(r, \phi, -L)\hat{\mathbf{z}}$, which is readily seen to have $H^W(\mathbf{B}') = 0$. We can use \mathbf{B}' to prove that the potential field \mathbf{B}^p also has $H^W(\mathbf{B}^p) = 0$ for a periodic field.

Our strategy is to prove that $H_{\mathbf{B}'}(\mathbf{B}^p) = 0$. Since we know that $H^W(\mathbf{B}^v) = 0$, we can then use Equation (57) to conclude that $H^W(\mathbf{B}^p) = 0$. To calculate $H_{\mathbf{B}'}(\mathbf{B}^p)$, let

$$\mathbf{B}^p = \nabla \left(\frac{\partial \psi}{\partial z} + B_0 z \right), \quad \text{where } \nabla^2 \psi = 0. \quad (62)$$

This representation is general and lets us write the vector potential (in cylindrical coordinates) as

$$\mathbf{A}^p = \nabla \times (\psi \hat{\mathbf{z}}) + \frac{r B_0}{2} \mathbf{e}_\phi. \quad (63)$$

(A similar representation in spherical coordinates was used by van Ballegoijen et al. 2000.) For the reference field, we choose the gauge $\mathbf{A}^v(r, \phi, z) = A_\phi^p(r, \phi, -L)\mathbf{e}_\phi$. In these gauges, we have

$$H_{\mathbf{B}'}(\mathbf{B}^p) = \int_V \mathbf{A}^p \cdot \mathbf{B}^p d^3x + \oint_{\partial V} \mathbf{A}^p \times \mathbf{A} \cdot \mathbf{n} d^3x. \quad (64)$$

The first term gives

$$\int_V \mathbf{A}^p \cdot \mathbf{B}^p d^3x = \int_V \left(\nabla \times (\psi \hat{\mathbf{z}}) + \frac{r B_0}{2} \mathbf{e}_\phi \right) \cdot \nabla \left(\frac{\partial \psi}{\partial z} + B_0 z \right) d^3x, \quad (65)$$

$$= \oint_{\partial V} \left(\frac{\partial \psi}{\partial z} + B_0 z \right) \mathbf{n} \cdot (\nabla \psi) \times \hat{\mathbf{z}} d^2x, \quad (66)$$

$$= \int_{S_s} \left(\frac{\partial \psi}{\partial z} + B_0 z \right) \frac{\partial \psi}{\partial \phi} d\phi dz, \quad (67)$$

$$= \int_{S_s} \frac{\partial \psi}{\partial z} \frac{\partial \psi}{\partial \phi} d\phi dz + B_0 \int_{-L}^L z \left(\int_0^{2\pi} \frac{\partial \psi}{\partial \phi} d\phi \right) dz. \quad (68)$$

The last integral vanishes by periodicity in ϕ . The surface integral in (64) vanishes on S_s due to our choices of gauge, leaving

$$\oint_{\partial V} \mathbf{A}^p \times \mathbf{A} \cdot \mathbf{n} d^3x = \int_{S_h-S_0} A_r^p A_\phi^v d^2x, \quad (69)$$

$$= \int_{S_h-S_0} A_r^p A_\phi^p d^2x, \quad (70)$$

$$= \int_{S_h-S_0} \frac{1}{r} \frac{\partial \psi}{\partial \phi} \left(-\frac{\partial \psi}{\partial r} + \frac{r B_0}{2} \right) r d\phi dr, \quad (71)$$

$$= - \int_{S_h-S_0} \frac{\partial \psi}{\partial \phi} \frac{\partial \psi}{\partial r} d\phi dr + \frac{B_0}{2} \int_0^{R_0} r \left(\int_0^{2\pi} \frac{\partial \psi}{\partial \phi} d\phi \right) dr. \quad (72)$$

Again the last term vanishes by periodicity in ϕ . Overall, we are left with

$$H_{\mathbf{B}^p}(\mathbf{B}^p) = \int_{S_s} \frac{\partial \psi}{\partial z} \frac{\partial \psi}{\partial \phi} d\phi dz - \int_{S_h-S_0} \frac{\partial \psi}{\partial \phi} \frac{\partial \psi}{\partial r} d\phi dr. \quad (73)$$

In fact, each of these integrals vanish. To see this, note that, since $\nabla^2 \psi = 0$, the derivatives inside the integrals may each be written as a Fourier series of the form

$$\frac{\partial \psi}{\partial r} = \sum_m f_m(r, z) (A_m \sin(m\phi) + B_m \cos(m\phi)). \quad (74)$$

By orthogonality of the trigonometric functions, products for different m vanish and we are left with integrals of the form

$$\begin{aligned} & \sum_m \int_{-L}^L m g_m(r, z) \left(\int_0^{2\pi} (A_m \sin(m\phi) + B_m \cos(m\phi)) \right. \\ & \quad \times (A_m \cos(m\phi) - B_m \sin(m\phi)) d\phi \Big) dz \end{aligned} \quad (75)$$

(and similar with z replaced by r). However, these integrals also vanish when integrated between 0 and 2π . Therefore $H_{\mathbf{B}^p}(\mathbf{B}^p) = 0$, and it follows that $H^W(\mathbf{B}^p) = 0$ for a periodic field in a cylindrical domain.

5.2.2. Aperiodic Boundary Conditions

If the magnetic field is aperiodic, i.e., $B_z(r, \phi, L) \neq B_z(r, \phi, -L)$, then the proof in Section 5.2.1 fails because there is no longer a straight, vertical magnetic field that matches the boundary conditions. In fact, for an aperiodic potential field, one might expect that the differing boundary conditions on S_0 and S_h could introduce a “twist,” in the sense of a net winding measured with respect to a fixed frame. To show that this is indeed the case, we present a specific example, studied previously by Janse & Low (2009) and Low (2011). Let \mathbf{B}^p be the specific field defined by the potential

$$\psi(r, \phi, z) = \frac{J_1(k_0 r)}{k_0^2} \left(\frac{\sinh(k_0 z)}{\sinh(k_0 L)} \sin \phi + \frac{3 \cosh(k_0 z)}{2 \cosh(k_0 L)} \cos \phi \right), \quad (76)$$

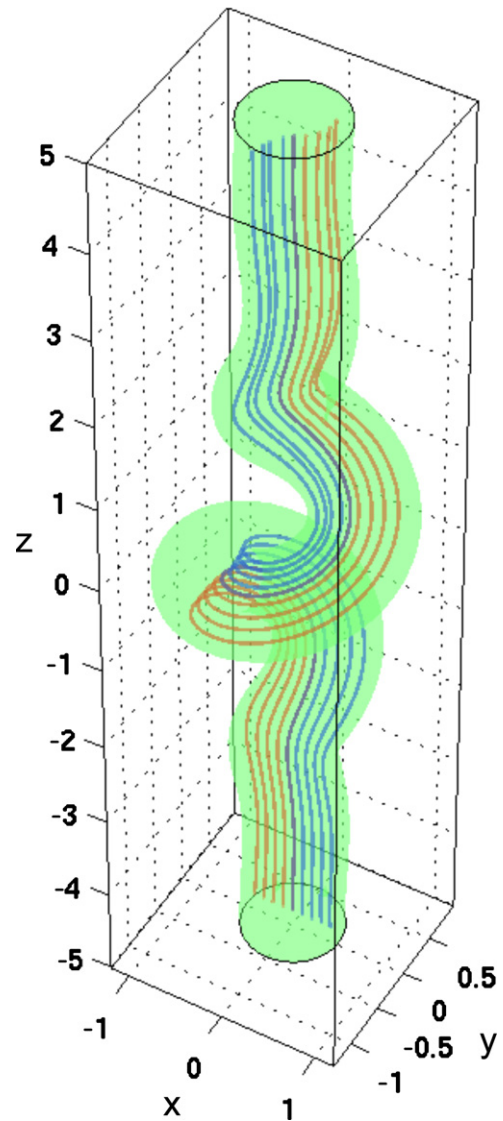


Figure 7. Potential field in a coiled domain, calculated using a finite-element method. Selected field lines show that this potential field is uniformly twisted, at a rate corresponding to the writhe of the axis curve. Consequently it has non-zero winding helicity $H^W(\mathbf{B}) \approx 0.16$.

(A color version of this figure is available in the online journal.)

as in Equation (62), and let $R_0 = L = 1$. Here J_1 is a Bessel function of the first kind, and the constant k_0 must be chosen so that $B_r|_{S_s} = 0$, which requires that $R_0 k_0 J_0(k_0 R_0) - J_1(k_0 R_0) = 0$. We take the smallest solution $k_0 \approx 1.8412$. This results in different distributions of B_z on S_0 and S_h , namely

$$B_z(r, \phi, -L) = 1.3 + J_1(k_0 r)(1.5 \cos \phi - \sin \phi), \quad (77)$$

$$B_z(r, \phi, L) = 1.3 + J_1(k_0 r)(1.5 \cos \phi + \sin \phi). \quad (78)$$

These are shown in Figure 6(a), along with a selection of field lines. The asymmetry between the two boundaries introduces a visible “twist” into the overall field, despite the fact that $\nabla \times \mathbf{B}^p \equiv 0$. We have calculated the flux function \mathcal{A}^W for this field using Equation (39), by numerically computing the pairwise winding numbers between a sample of field lines. This is shown in Figure 6(b). Integrating this flux function over S_0 , weighted by $B_z(r, \phi, -L)$, we find that $H^W \approx -0.09$. For this particular example, our numerical H^W converges to the same

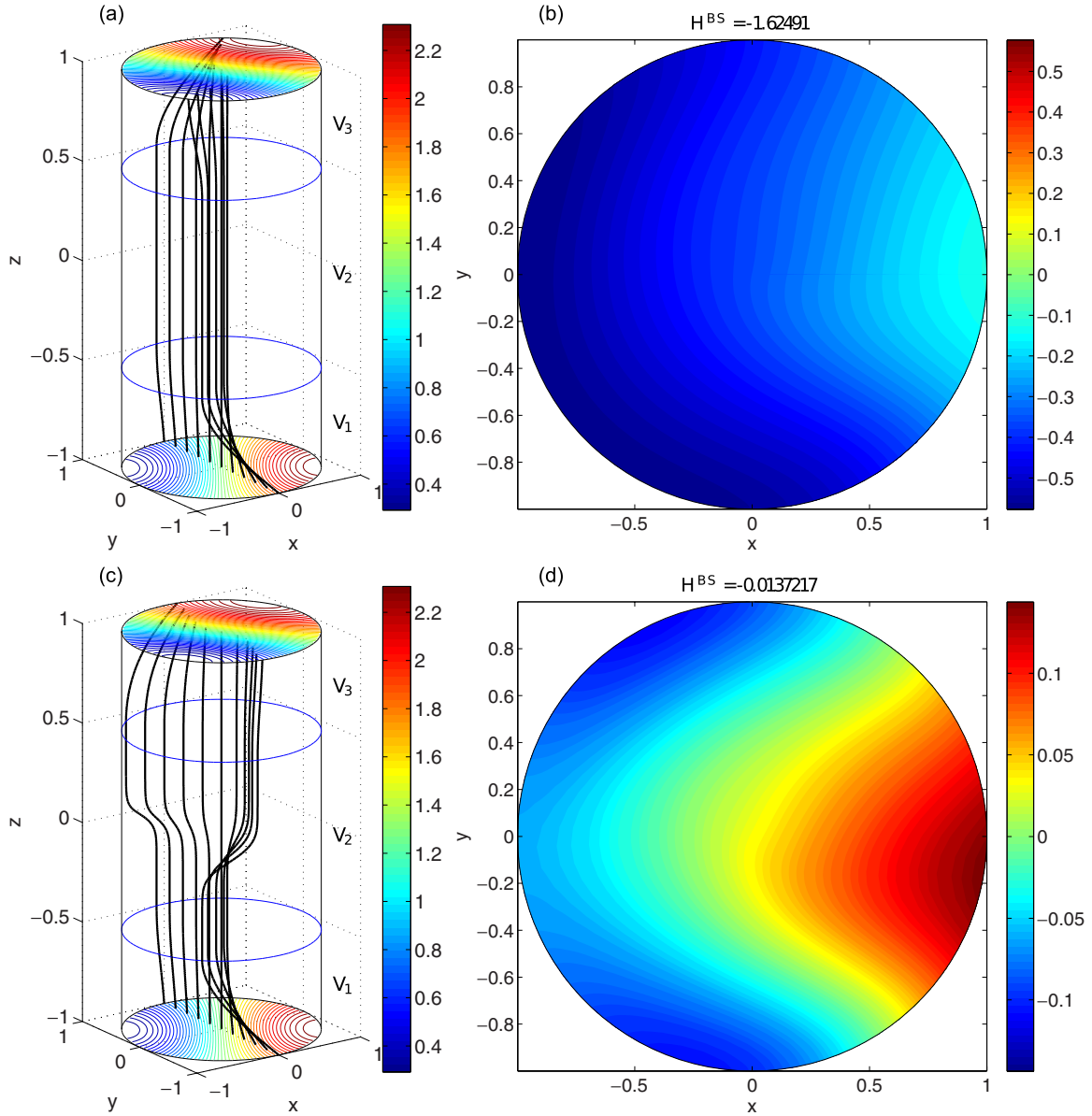


Figure 8. Magnetic field with $H^W = 0$, constructed according to the method in Appendix A. Panels (a), (b) show the magnetic field and \mathcal{A}^W for $k = 0$, while panels (c), (d) show corresponding plots for a non-zero value of k , chosen so that $H^W \approx 0$. Here we took $R_0 = L = 1$, $z_1 = -0.5$, $z_2 = 0.5$.

(A color version of this figure is available in the online journal.)

value as the cylindrical helicity defined by Low (2011), which for this field is

$$H = -\frac{6\pi L J_1^2(k_0 R_0)}{k_0^2 \sinh(k_0 L)}. \quad (79)$$

However, as we show in Appendix B, the gauge \mathbf{A}^{CK} used by Low differs, in general, from \mathbf{A}^W . Therefore they are measuring winding with respect to different frames.

In summary, this example shows that an aperiodic potential field may have non-zero H^W . In Section 5.3, we will see one way of constructing an alternative field that has $H^W = 0$.

5.2.3. Twisted Domains

Even if the boundary conditions are periodic, the potential field may inherit winding due to the shape of the domain. Figure 7 shows an example where the potential field has non-zero H^W owing to the coiled shape of the domain, despite

the fact that we have uniform boundary conditions $B_z = 1$ on both S_0 and S_h . Up to an integer, $\mathcal{L}(\mathbf{x}, \mathbf{y})$ is the difference $\Theta(\mathbf{x}, \mathbf{y})(h) - \Theta(\mathbf{x}, \mathbf{y})(0)$, and it may be seen from the field lines plotted in Figure 7 that the field is uniformly twisted (i.e., $\mathcal{L}(\mathbf{x}, \mathbf{y})$ is the same for all pairs of field lines). As this domain is tubular, we can decompose H^W into the sum of twisting \mathcal{T} (the rotation of field lines about the central axis of the tube), and writhing \mathcal{W} (a quantity measuring the self-winding of the tube's axis); see Berger & Prior (2006). Here we have numerically confirmed that the helicity H^W of the domain is equal to the writhe \mathcal{W} , and hence $\mathcal{T} = 0$, meaning that the field has no internal twist about its axis. The writhing is a property of the axis shape alone, so in this case the potential-field helicity H^W is entirely determined by the shape of the domain. In general, aperiodic boundary conditions and/or non-potential fields on such domains will also have internal helicity from the twisting and braiding of field lines along the tube's length. It is possible for a field to

have $H^W = 0$ on such a domain, but in this case it would require some internal twisting, unlike the cylindrical domain.

5.3. Equivalence of relative helicity and standard helicity

In what follows we once again restrict ourselves to a circular cylinder $V = \{0 \leq r \leq R_0, 0 \leq \phi < 2\pi, -L \leq z \leq L\}$ to provide clarity to the arguments. To substantiate our claim that the standard magnetic helicity and the relative helicity have equal physical meaning, we can use Equation (57) to prove that the gauge choice in $H(\mathbf{B})$ and the choice of \mathbf{B}' in $H_{\mathbf{B}'}(\mathbf{B})$ are equivalent. Our result may be formulated as follows.

1. *Given any reference field \mathbf{B}' , we can always find a gauge in which $H(\mathbf{B}) = H_{\mathbf{B}'}(\mathbf{B})$.*
2. *Conversely, given an arbitrary gauge for $H(\mathbf{B})$, we can always find \mathbf{B}' such that $H_{\mathbf{B}'}(\mathbf{B}) = H(\mathbf{B})$.*

To prove part 1, note that in any gauge we can write

$$H(\mathbf{B}) = H^W(\mathbf{B}) + \int_{S_h} \chi B_z d^2x - \int_{S_0} \chi B_z d^2x, \quad (80)$$

where $\mathbf{A} = \mathbf{A}^W + \nabla\chi$. From Equation (57) we know that $H_{\mathbf{B}'}(\mathbf{B}) = H^W(\mathbf{B}) - H^W(\mathbf{B}')$, so we can simply choose the gauge to be

$$\chi = -\left(\frac{z+L}{2L\Phi_0}\right) H^W(\mathbf{B}'), \quad (81)$$

which is a function of z only. To prove part 2, note that we can give $H(\mathbf{B})$ an arbitrary real value by changing gauge. Applying Equation (57) again, we must then show the existence of a reference field \mathbf{B}' such that $H^W(\mathbf{B}')$ takes any arbitrary value. We show one way to explicitly construct such a reference field in Appendix A.

One application of the technique in Appendix A is to construct a reference field with vanishing H^W . To illustrate such a construction, let V be the same circular cylinder as in Section 5.2, and take the same boundary conditions (77), (78) as for the potential field in Section 5.2.2. That potential field was “twisted,” with $H^W \neq 0$. By choosing the arbitrary constant k appropriately in the field \mathbf{B}_k (see Appendix A), we can construct an alternative magnetic field with $H^W = 0$. For this example, we have chosen $z_1 = -0.5$, $z_2 = 0.5$, and $f(z) = \exp(-100z^2)$. The constructed fields with $k = 0$ and with the (roughly) optimum value of $k \approx 4.14$ are shown in Figure 8. This field is likely not the only possible field with $H^W = 0$ (even its topology, as captured by the \mathcal{A}^W distribution, is likely not unique). Nor is it likely to be a stable equilibrium. It is presented here simply to prove that a field with $H^W = 0$ exists for arbitrary boundary conditions on the cylinder. Note that while $H^W = 0$, indicating that the average pairwise winding of the field lines vanishes, it is clear that $\mathcal{A}^W \neq 0$, so that individual field lines do see a net winding.

6. CONCLUSIONS

To summarize, we have shown that, for open magnetic fields between two parallel planar boundaries, the helicity H has a physical meaning in any gauge: it is the average pairwise winding number of magnetic field lines with respect to some frame field. We have shown how this gauge freedom is equivalent to the freedom of choice of reference field in the commonly used relative helicity for such fields. Moreover, there is a unique choice of gauge that always measures winding with respect to a fixed frame. This is the “winding” gauge of

Equation (18). We propose that the helicity in this gauge (H^W) is a physically motivated measure of the topological linking in an open magnetic field, that is uniquely defined and does not depend on choice of an arbitrary reference field. In effect, it always measures winding with respect to a straight field. As we have demonstrated in Section 4.2, from a geometrical perspective any other choice is unnecessary as it adds a contribution to the helicity arising from the rotation of the reference frame used to measure winding. This quantity has no physical meaning. Using the relative helicity with a potential reference field may or may not measure the same helicity H^W , depending on the boundary conditions. If it differs from H^W then the relative helicity measure necessarily includes a contribution due to a rotating reference frame.

As a result, we make the following practical recommendation. In magnetic fields having more than one boundary with $B_n \neq 0$, one should calculate H^W , rather than using the relative helicity with potential field as a reference. For a cylindrical domain whose end boundaries S_0 and S_h are the same shape, and if the boundary conditions on B_n are the same on both ends (i.e. are periodic), then the two helicities are equal. This is because the potential field itself then has vanishing H^W in such a field, meaning that it is untwisted with respect to a straight field. However, if these conditions are not met then the potential field will generally have $H^W \neq 0$, so that the relative helicity does not match H^W . For example, we have shown that this may arise if the boundary conditions are aperiodic (Section 5.2.2) or if the domain boundary has a complex shape (5.2.3). We envisage that the absolute measure provided by H^W will be particularly useful when analyzing the time evolution of magnetic configurations where B_n on the boundary is changing, or when comparing different magnetic fields. An example of the latter would be the comparison of different magnetic active regions in the solar corona (Valori et al. 2012).

In practical terms, there are several ways to calculate $H^W(\mathbf{B})$ for a given magnetic field \mathbf{B} . Using (57), one can calculate the relative helicity with respect to a reference field known to have vanishing H^W (for example, Appendix A shows how to construct such a reference in the cylinder). Or, one can evaluate the vector potential by numerically evaluating (18), then computing $\int_V \mathbf{A}^W \cdot \mathbf{B} d^3x$. But the most straightforward method will generally be to utilize the physical interpretation and calculate H^W directly from \mathbf{B} using (34), evaluating pairwise winding numbers of field lines. We have implemented this numerically for the examples in Figures 6 and 8.

It is interesting to observe that there are some similarities between the winding gauge choice and the gauges chosen by Hornig (2006) and by Low (2011) in their suggested “universal” or “absolute” helicities. Hornig (2006) fixes H with the gauge condition that $\nabla^\perp \cdot \mathbf{A} = 0$ everywhere on the boundary ∂V (here ∇^\perp denotes the component of the gradient tangential to the boundary). On S_0 and S_h , this condition is satisfied by \mathbf{A}^W (this is seen directly from Equation (21)), but it is not satisfied in general by \mathbf{A}^W on S_s . Low (2011) defines an absolute helicity H (for V a cylinder) by taking the gauge

$$\mathbf{A}^{\text{CK}} = \nabla \times \psi \hat{\mathbf{z}} + \eta \hat{\mathbf{z}}, \quad (82)$$

which corresponds to a Chandrasekhar–Kendall representation of \mathbf{B} for functions ψ , η . Our \mathbf{A}^W may also be written in this form with

$$\psi = -\frac{1}{2\pi} \int_{S_s} B_z(\mathbf{y}) \log |\mathbf{r}| d^2y, \quad \eta = A_z^W. \quad (83)$$

However, Low applies specific boundary conditions to uniquely define ψ and η , and these are not the same as for \mathbf{A}^W in general (see Appendix B). Another gauge condition, suggested by Valori et al. (2012), is that $A_z = 0$; this does not uniquely specify the gauge, and the resulting freedom is used to make $H_{B^*} \equiv H$. However, we show in Appendix B that the winding gauge \mathbf{A}^W may have $A_z^W \neq 0$, so in general this measure differs from H^W . We conclude in general that these proposed gauges measure the field-line winding in a non-physical rotating frame, yielding (in general) a different helicity measure from H^W .

We conclude with some remarks about the generality of our results. We have assumed that our domain V is simply connected and lies between two parallel planar boundaries S_0 , S_h . Furthermore, these parallel boundaries are the only part of the boundary where we allow $B_n \neq 0$. These restrictions are necessary so that the winding gauge \mathbf{A}^W is well-defined. In making the restriction that S_0 and S_h are planar and parallel, we are essentially identifying a distinguished direction ($\hat{\mathbf{z}}$) that is perpendicular to the cross-sections S_z on which \mathbf{A}^W is defined. This distinguished direction is also needed for defining winding numbers $\mathcal{L}(\mathbf{x}, \mathbf{y})$, along with a choice of coordinate frame $\{\hat{\mathbf{e}}_1, \hat{\mathbf{e}}_2\}$ on each cross-section. Extending the definitions of \mathbf{A}^W or \mathcal{L} to a domain with curved boundaries S_0 , S_h would require choosing a foliation of curved cross-sectional surfaces throughout V , complicating the definition of what it means for two curves to have non-zero winding number. We hope to address these complications in future.

A.R.Y. was supported by STFC consortium grant ST/K001043/1 to the universities of Dundee and Durham, and C.P. by an Addison-Wheeler postdoctoral fellowship. We thank the referee for interesting suggestions that have improved the paper. Figure 7 used iFEM (Chen 2009) and DistMesh (Persson & Strang 2004).

APPENDIX A CONSTRUCTION OF A MAGNETIC FIELD WITH ARBITRARY H^W

In this Appendix, we give one method for constructing a magnetic field \mathbf{B} in a circular cylinder V to match arbitrary normal distributions on S_0 and S_h which have a non-zero net flux, such that $H^W(\mathbf{B})$ is an arbitrary real number. Denote the two normal distributions by $B_z|_{S_0} = g_0(x, y)$ and $B_z|_{S_h} = g_h(x, y)$. We assume that $B_r|_{S_0} = 0$, so conservation of flux requires that $\int_{S_0} g_0 d^2x = \int_{S_h} g_h d^2x$. We begin by assuming that B_z can only have one sign on both boundaries, that is to say $g_0(x, y)$ and $g_h(x, y)$ are either both positive definite or both negative definite.

The basic idea of our construction is to divide V into three distinct subdomains $V_1 = V \cap \{z | z \in [-L, z_1]\}$, $V_2 = V \cap \{z | z \in [z_1, z_2]\}$, and $V_3 = V \cap \{z | z \in [z_2, L]\}$. We utilise the property that H^W is additive in z , i.e.,

$$H^W(V) = H^W(V_1) + H^W(V_2) + H^W(V_3). \quad (\text{A1})$$

This follows from the winding-number interpretation in Section 4. In V_2 we will choose a magnetic field whose winding helicity is known and can be controlled. In V_1 and V_3 we will show how to construct magnetic fields that map the boundary flux distributions (on S_0 and S_h) to uniform flux distributions on the intermediate surfaces S_{z_1} and S_{z_2} , so as to match on to the chosen field in V_2 . These two fields will contribute some

fixed $H^W(V_1) + H^W(V_3)$ that depends only on g_0 , g_h , and not on the choice of field in V_2 . By choosing the field in V_2 appropriately, we will obtain any desired $H^W(V_2)$ and hence any desired $H^W(V)$. An example magnetic field computed with this method is shown in Figure 8.

1. *Volume V_2 .* In this region, we shall set

$$\mathbf{B}(V_2) = \mathbf{B}_0 + \mathbf{B}_k, \quad (\text{A2})$$

where $\mathbf{B}_0 = B_0 \hat{\mathbf{z}}$ and $\mathbf{B}_k = kf(z)(-x_2 \hat{\mathbf{e}}_1 + x_1 \hat{\mathbf{e}}_2)$. Here k is an arbitrary constant, $f(z)$ is an arbitrary function of z (for now), and (x_1, x_2, z) are Cartesian coordinates. This field corresponds to an overall twist that varies in z . Let \mathbf{A}_0 and \mathbf{A}_k be vector potentials for \mathbf{B}_0 and \mathbf{B}_k in the winding gauge. Then

$$H^W(V_2) = \int_{V_2} (\mathbf{A}_0 + \mathbf{A}_k) \cdot (\mathbf{B}_0 + \mathbf{B}_k) d^3x. \quad (\text{A3})$$

From the definitions of \mathbf{B}_0 , \mathbf{B}_k and the winding gauge, we have immediately that $\mathbf{A}_0 \cdot \mathbf{B}_0 = 0$ and $\mathbf{A}_k \cdot \mathbf{B}_k = 0$. We also find that

$$\mathbf{A}_0 \cdot \mathbf{B}_k = \frac{kB_0 f(z)}{2\pi} \int_{S_z} \frac{x_2(x_2 - y_2) + x_1(x_1 - y_1)}{(x_1 - y_1)^2 + (x_2 - y_2)^2} d^2y, \quad (\text{A4})$$

$$\mathbf{A}_k \cdot \mathbf{B}_0 = \frac{kB_0 f(z)}{2\pi} \int_{S_z} \frac{-y_2(x_2 - y_2) - y_1(x_1 - y_1)}{(x_1 - y_1)^2 + (x_2 - y_2)^2} d^2y. \quad (\text{A5})$$

Therefore, we get an explicit expression for the winding helicity

$$H^W(V_2) = \frac{\pi k B_0 R_0^4}{2} \int_{z_1}^{z_2} f(z) dz. \quad (\text{A6})$$

In particular, by varying k we may obtain any real value for $H^W(V_2)$. We shall choose the function $f(z)$ so that \mathbf{B}_k matches smoothly to zero at $z = z_1$ and $z = z_2$.

2. *Volumes V_1 and V_3 .* It suffices to consider V_1 (a similar construction will work in V_3). Our strategy is to first prescribe B_z to be some function $\lambda(r, \phi, z)$ that interpolates between $\lambda(r, \phi, -L) = g_0(r, \phi)$ and $\lambda(r, \phi, z_1) = B_1$ (constant), then find suitable B_r , B_ϕ such that $\nabla \cdot \mathbf{B} = 0$. (We work in polar coordinates.) For this, it is convenient to write $\mathbf{B} = \lambda \mathbf{v}$, where $\mathbf{v} = v_r(r, \phi, z) \mathbf{e}_r + v_\phi(r, \phi, z) \mathbf{e}_\phi + \hat{\mathbf{z}}$. Then from $\nabla \cdot \mathbf{B} = 0$ we get

$$\frac{1}{\lambda} \frac{d\lambda}{dz} = -\nabla \cdot \mathbf{v}, \quad (\text{A7})$$

where the derivative is taken along field lines $r(z)$, $\phi(z)$ (cf. Yeates et al. 2012). The chain rule gives

$$\frac{\partial \ln \lambda}{\partial r} v_r + \frac{1}{r} \frac{\partial \ln \lambda}{\partial \phi} v_\phi + \frac{\partial \ln \lambda}{\partial z} = -\frac{1}{r} \frac{\partial}{\partial r} (r v_r) - \frac{1}{r} \frac{\partial v_\phi}{\partial \phi}. \quad (\text{A8})$$

Since we have one equation for the two unknowns v_r , v_ϕ , there is some freedom remaining. In order to satisfy $B_r = 0$ on the side boundary S_s , we shall simply choose $v_r \equiv 0$ throughout V . (This means that all field lines of our constructed field will lie on concentric cylinders.) In that case, (A8) reduces to

$$\frac{\partial \ln \lambda}{\partial \phi} v_\phi + r \frac{\partial \ln \lambda}{\partial z} = -\frac{\partial v_\phi}{\partial \phi}. \quad (\text{A9})$$

At fixed r, z , this is an ordinary differential equation, readily solved to find

$$v_\phi(r, \phi, z) = \frac{\lambda(r, \phi, z)}{\lambda(r, 0, z)} \left(v_\phi(r, 0, z) - \frac{1}{\lambda(r, 0, z)} \int_0^\phi r \frac{\partial \lambda}{\partial z} d\phi \right). \quad (\text{A10})$$

For each r and z , the value $v_\phi(r, 0, z)$ is an arbitrary constant; we may set all of these to zero. Finally, we shall impose the additional requirement on λ that $\partial \lambda / \partial z|_{S_{z_1}} = 0$. This will ensure that $v_\phi = 0$ on S_{z_1} , so that our magnetic field in V_1 continuously matches to that in V_2 . Our construction is completed by finding a suitable interpolant $\lambda(r, \phi, z)$. For each r, ϕ , we may choose λ to be the unique quadratic function $Q(z)$ such that $Q(-L) = g_0(r, \phi)$, $Q(z_1) = B_1$, $Q'(z_1) = 0$. This is

$$\lambda(r, \phi, z) = B_1 + \frac{(z_1 - z)^2}{(z_1 + L)^2} (g_0(r, \phi) - B_1). \quad (\text{A11})$$

Finally we note that, since the value of the helicities on $H^W(V_1)$ and $H^W(V_3)$ have no dependence on k , we can simply choose k such that $H^W(V)$ takes any desired value.

We now relax our assumption on the sign of the functions g_0 and g_h , allowing both signs, although our construction will require that the net flux $\int_{S_0} g_0 d^2x$ is non-zero. The field representation $\lambda \mathbf{v}$ is not valid where the function λ is zero and consequently our argument on the domains V_1 and V_3 for mapping the B_z distributions from g_0 and g_h to a constant on the planes S_{z_1} , S_{z_2} breaks down. To remedy this, we observe that the argument has no essential dependence on the relative size of the three domains. Thus we shrink the domain $V_1 \cup V_2 \cup V_3$ to allow for an additional domain at each end, i.e., $V_0 = V \cap \{z | z \in [-L, z_a]\}$, $V_1 = V \cap \{z | z \in [z_a, z_1]\}$, $V_2 = V \cap \{z | z \in [z_1, z_2]\}$, $V_3 = V \cap \{z | z \in [z_2, z_b]\}$ and $V_4 = V \cap \{z | z \in [z_b, L]\}$. On the domain V_0 we set \mathbf{B} to be the unique potential field satisfying $B_r = 0$ on S_s , $B_z = g_0$ on S_0 , and $B_z = B_1$ (constant) on S_{z_a} . Similarly, on V_4 we set \mathbf{B} to be the equivalent potential field with $B_z = B_1$ on S_{z_b} . The same construction as before may then be used on V_1, V_2 , and V_3 . Since

$$H^W(V) = \sum_{i=0}^4 H^W(V_i), \quad (\text{A12})$$

and only $H^W(V_2)$ depends on k , we can simply alter k to obtain any desired value of $H^W(V)$.

APPENDIX B

DEMONSTRATING $\mathbf{A}^{\text{CK}} \neq \mathbf{A}^{\text{W}}$ WITH LOW'S SPECIFICATION OF ψ

The gauge choice used by Low (2006, 2011) in (82) is such that the function $\eta \equiv A_z^{\text{CK}}$ is zero on the boundary of the discs S_z . We demonstrate here that there is at least one admissible field on the cylinder for which $A_z^{\text{W}} \neq 0$ at some point on the boundary S_s , so that $\mathbf{A}^{\text{CK}} \neq \mathbf{A}^{\text{W}}$. The field

$$\mathbf{B} = -x_2^2 \hat{\mathbf{e}}_1 + x_1 x_2 \hat{\mathbf{e}}_2 + (B_0 - x_1 z) \hat{\mathbf{z}}. \quad (\text{B1})$$

is divergence free and tangent to the side boundary of the cylinder. At the particular point $(0, -R_0)$ on the side boundary, one may show by direct calculation that $A_z^{\text{W}}(0, -R_0) = R_0^3/8$.

REFERENCES

- Arnol'd, V. I. 1986, *Sel. Math. Sov.*, 5, 327
 Arnol'd, V. I., & Khesin, B. A. 1998, *Topological Methods in Hydrodynamics* (New York: Springer)
 Berger, M. A. 1986, *GAFD*, 34, 265
 Berger, M. A. 1993, *PRL*, 70, 705
 Berger, M. A., & Field, G. B. 1984, *JFM*, 147, 133
 Berger, M. A., & Prior, C. 2006, *JPhA*, 39, 8321
 Brown, M., Canfield, R., Field, G., et al. 1999, *Washington DC American Geophysical Union Geophysical Monograph Series*, 111, 301
 Cantarella, J., Deturck, D., & Gluck, H. 2001, *JMaPh*, 42, 876
 Chen, L. 2009, *iFEM: an Integrated Finite Element Methods Package in MATLAB*, Technical Report, University of California at Irvine
 Démoulin, P. 2006, *AdSpR*, 37, 1269
 Démoulin, P. 2007, *AdSpR*, 39, 1674
 Démoulin, P., Parlat, E., & Berger, M. A. 2006, *SoPh*, 233, 3
 Finn, J. H., & Antonsen, T. M. J. 1985, *CoPPC*, 9, 111
 Hornig, G. 2006, *arXiv:astro-ph/0606694*
 Janse, A. M., & Low, B. C. 2009, *ApJ*, 690, 1089
 Jensen, T. H., & Chu, M. S. 1984, *PhFl*, 27, 2881
 Longcope, D. W., & Malanushenko, A. 2008, *ApJ*, 674, 1130
 Low, B. C. 2006, *ApJ*, 646, 1288
 Low, B. C. 2011, *PhPl*, 18, 052901
 Moffatt, H. K. 1969, *JFM*, 35, 117
 Moffatt, H. K., & Ricca, R. L. 1992, *RSPSA*, 439, 411
 Persson, P.-O., & Strang, G. 2004, *SIAMR*, 46, 329
 Ricca, R. L., & Nipoti, B. 2011, *J. Knot. Th. Ram.*, 20, 1325
 Valori, G., Démoulin, P., & Parlat, E. 2012, *SoPh*, 278, 347
 van Ballegoijen, A. A., Priest, E. R., & Mackay, D. H. 2000, *ApJ*, 539, 983
 Webb, G. M., Hu, Q., Dasgupta, B., & Zank, G. P. 2010, *JGRA*, 115, 10112
 Yeates, A. R., & Hornig, G. 2013, *PhPl*, 20, 012102
 Yeates, A. R., Hornig, G., & Welsch, B. T. 2012, *A&A*, 539, A1